第 35 卷第 8 期 无 机 化 学 学 报 Vol.35 No.8
2019 年 8 月 CHINESE JOURNAL OF INORGANIC CHEMISTRY 1470-1476

在紫外和可见光下具有高催化活性的珊瑚状金红石型二氧化钛的制备

朱 捷*,[1] 葛奉娟[1] 陈 艳[1] 徐 艳[1] 张学杨[2] 邹伟欣[3] 董 林*,[3]
([1]徐州工程学院化学化工学院,徐州 221111)
([2]徐州工程学院环境工程学院,徐州 221111)
([3]介观化学教育部重点实验室,南京大学化学化工学院,南京 210093)

摘要:采用溶剂热法在二乙二醇溶液中制备了珊瑚状的金红石二氧化钛(Rut-dg)。扫描电子显微镜(SEM)和 X 射线衍射(XRD)表明样品呈均匀分散的球形颗粒,直径约为 1 μm,表面具有珊瑚状的突起结构,半径约 10 nm。氮气吸附-脱附结果表明样品比表面达到 228 $m^2 \cdot g^{-1}$, 是商品金红石的 7 倍多。由于其特殊的形貌,Rut-dg 在紫外光下的催化产氢量达到 25 000 $\mu mol \cdot g^{-1} \cdot h^{-1}$,比 P25 高出 50%,是商品金红石活性的 13 倍。在可见光下的产氢量为 270 $\mu mol \cdot g^{-1} \cdot h^{-1}$,而 P25 和商品金红石则没有明显活性。进一步实验表明,Rut-dg 样品表面检测不到可能引起活性增加的有机杂质存在,因此,珊瑚状的形貌是影响活性的重要因素。样品在 300 ℃焙烧后,珊瑚状表面结构明显烧结,比表面下降了 50%,导致产氢量下降了 15%~25%,这也说明珊瑚状结构大大促进了光催化产氢活性的提高。

关键词:水热法;金红石二氧化钛;多相催化;分解水;光分解;产氢
中图分类号:O644.1 **文献识别码**:A **文章编号**:1001-4861(2019)08-1470-07
DOI:10.11862/CJIC.2019.162

Preparation of Coral-like Rutile Titania with Enhanced Photocatalytic Activity under UV and Visible Light

ZHU Jie*,[1] GE Feng-Juan[1] CHEN Yan[1] XU Yan[1] ZHANG Xue-Yang[2] ZOU Wei-Xin[3] DONG Lin*,[3]
([1]*School of Chemistry and Chemical Engineering, Xuzhou University of Technology, Xuzhou, Jiangsu* 221111, *China*)
([2]*School of Environmental Engineering, Xuzhou University of Technology, Xuzhou, Jiangsu* 221111, *China*)
([3]*Key Laboratory of Mesoscopic Chemistry of MOE, School of Chemistry and Chemical Engineering, Nanjing University, Nanjing* 210093, *China*)

Abstract: Coral-like rutile titania (Rut-dg) was synthesized by solvothermal method in diethylene glycol solution. Scanning electron microscope (SEM) and X-ray diffraction (XRD) indicated the spherical particles were homogeneously dispersed with the diameter about 1 μm, consisting regular arranged branches on the surface with diameter less than 10 nm. The BET surface area was as large as 228 $m^2 \cdot g^{-1}$, more than 7 times of commercial rutile titania sample. Given its unique morphology, the Rut-dg showed superior photocatalytic activity with hydrogen evolution 25 000 $\mu mol \cdot g^{-1} \cdot h^{-1}$ under ultraviolet irradiation, 50% higher than P25 and 13 times of commercial rutile sample. The hydrogen production under visible light was 270 $\mu mol \cdot g^{-1} \cdot h^{-1}$, while P25 and commercial rutile had no obvious activity. Further investigation demonstrated that no organics could be detected on the surface of Rut-dg, indicating the coral-like structures played the key role for the photocatalytic activity. After calcined at 300 ℃, the coral-like structures were sintered obviously and the surface area decreased by

收稿日期:2019-01-21。收修改稿日期:2019-05-22。
徐州市重点研发计划(社会发展)项目(No.KC17154)资助。
*通信联系人。E-mail:zhujie19@qq.com, donglin@nju.edu.cn

50%. Meanwhile, the hydrogen production decreased by 15%~25%, also implying that the coral-like structures facilitated the hydrogen production dramatically.

Keywords: solvothermal; rutile titania; heterogeneous catalysis; water splitting; photolysis; hydrogen generation

0 Introduction

With the development of modern industry, the depletion of fossil fuels and the environmental pollutions have become serious problems. The development of renewable and clean energies become one of the most emergent research subjects[1-2]. Conversion of solar energy into hydrogen (H_2) is considered as a perspective approach to solve these problems. Water splitting is an eco-friendly process that can be operated at ambient temperature and pressure[3-6]. Since 1972, Fujishima and Honda has reported photoassisted electrochemical water splitting on single-crystal titania and platinum electrodes[7], up to now, a large number of photocatalytic materials, with the enhanced light harvesting, photogenerated charge separation and transport, are designed for the photocatalytic hydrogen production, including binary metal oxides[8-14], complex metal oxides[15-18], metal sulfides[19-21] and metal-free materials[22-26].

TiO_2 has been widely used as a good photocatalyst in H_2 production from water splitting, due to its advantages of being cheap, stable, nontoxic and environmentally friendly. Generally, TiO_2 has four polymorphs, including anatase, rutile, brookite and TiO_2(B). These four polymorphs are used in different fields on the basis of their different physical and chemical properties, but the most frequently studied TiO_2 based photocatalysts are anatase and rutile. Anatase, as it has higher surface area, more oxygen vacancies and lower conduction band (CB) potential, usually has better photocatalytic activity. However, anatase has poor visible light adsorption, which limits its application. It is reported that rutile has narrower band gap and faster charge carrier mobile, which make it a good candidate for photocatalytic reactions. There are still some shortcomings for rutile TiO_2, such as lower surface area, less oxygen vacancies and faster e^--h^+ recombination[27]. Therefore, there are very few literatures that using pure rutile TiO_2 as photocatalysts, especially in hydrogen production field. Even for those anatase-rutile combined catalysts, the catalysts with best activity usually compose only a small part of rutile[28-32]. Particularly, the commercial catalyst P25 (Degussa) is composed of about 71% anatase and 29% rutile. On the other hand, the morphology of TiO_2 is an important factor for its photocatalytic activities. Some researchers prepared coral-like TiO_2 with anatase phase or anatase-rutile mixed phases which have higher discoloration rate of organic dye solution[33-34]. However, the hydrogen generation by water splitting was seldom reported. Herein, we prepared coral-like rutile TiO_2 in diethylene glycol solution by solvothermal method. The sample has high surface area and outstanding photocatalytic activities on H_2 production from water splitting.

1 Experimental

1.1 Chemicals

Titanium (Ⅳ) butoxide (TBOT, >99.0%), diethylene glycol (DG, >99.0%), chloroplatinic acid hexahydrate ($H_2PtCl_6 \cdot 6H_2O$, AR), triethanolamine (TEOA, 98%) and commercial rutile TiO_2 (Rut-c for short, 99.8%) were purchased from Aladdin. Hydrochloric acid (HCl, 36%~38% (*w*/*w*)) was purchased from Shanghai Lingfeng. P25 was purchased from Degussa Corporation.

1.2 Preparation of coral-like rutile TiO_2

The coral-like rutile TiO_2 was prepared by solvothermal method in reference[35] with some modification. In a typical synthesis, 2 mL TBOT was dissolved in 30 mL DG. After ultrasonication for 30 min, 10 mL HCl (5 $mol \cdot L^{-1}$) was added dropwise. The mixed solution was ultrasonicated for further 30 min before transferred into a 50 mL Teflon-lined stainless-steel autoclave. The autoclave was heated to 150 ℃ and maintained for 24 h. Then the autoclave was cooled down naturally to ambient temperature. The sample was centrifuged,

washed several times by deionized water (DI) and ethanol and dried at 80 ℃ overnight. The sample was denoted as Rut-dg. As comparison, the DG solution was replaced by ethanol or ethylene glycol, and the resulted samples were denoted as Rut-et and Rut-eg.

1.3 Characterization

Scanning electron microscopy (SEM) experiment was performed on a Philips XL30 electron microscope operated at beam energy of 10.0 kV. Transmission electron microscopy (TEM) images were taken on a JEM-2100 instrument at an acceleration voltage of 200 kV. The crystal structures were identified by X-ray diffraction (XRD) with Philips X′Pert Pro diffractometer by Ni-filtered Cu $K\alpha$ radiation (λ=0.154 18 nm). The X-ray tube was operated at 40 kV and 40 mA. The scanning range was 10°~80°. Brunauer-Emmet-Teller (BET) surface area was measured by nitrogen adsorption-desorption at 77 K on Micrometrics ASAP-2020 adsorption apparatus. The FT-IR spectra were collected from 400 to 4 000 cm^{-1} at the spectral resolution of 4 cm^{-1} on Nicolet 5700 FT-IR spectrometer. UV-Vis diffuse reflectance spectroscopy (UV-Vis DRS) were recorded in the range of 200~800 nm by a Shimadzu UV-2401 spectrophotometer with the reference of $BaSO_4$.

1.4 Hydrogen production test

The photocatalytic hydrogen evolution reaction was carried out in a top-irradiation vessel connected to a gas-closed glass system under an irradiation of 300 W Xe lamp with or without the 420 nm cut-off filter, to test the activity under visible or UV light. 50 mg catalyst was dispersed in 100 mL aqueous solution (90 mL DI water and 10 mL TEOA. H_2PtCl_6 aqueous solution was added which was *in-situ* reduced to Pt during the reaction (3%(*w*/*w*) Pt). The temperature of solution was kept around 6 ℃. The reaction system was sealed and evacuated for 30 min before irradiation. The amount of generated hydrogen was determined by a gas chromatograph.

2 Results and discussion

2.1 Morphology of Rut-dg

The morphology of Rut-dg was investigated by SEM. Fig.1(a,b) showed the spherical particles with uniform diameters at about 800~1 000 nm with coral-like surface. The intersecting surface of the broken spheres (Fig.1c) exhibited the radical pore passages in it, and the branches could be estimated to have a length of ~200 nm and a diameter of ~10 nm.

The phase structure of the Rut-dg was characterized by XRD (Fig.1d). The sample showed typical diffraction peaks at about 27.40°, 35.84°, 41.22° and 54.28°. Compared with PDF No.78-2485, the peaks correspond with the (110), (101), (111) and (211) planes of rutile TiO_2, respectively. Meanwhile, no peaks of anatase TiO_2 was observed, indicating that pure rutile structure was prepared by this method. According to Scherrer equation $D=K\gamma/(B\cos\theta)$, the mean particle size calculated though (110) plane diffraction peak was about 7.35 nm, where K is the Scherrer constant 0.89, B is the full width at half maximum (FWHM) at 2θ= 27.4°, λ is the wavelength of X ray (0.154 18 nm). Combined with the SEM result, this size should be the diameter of the coral branches.

The detailed structure of the coral branches was examined by TEM in Fig.1(e,f). It can be clearly seen that the diameters of the branches were about 7~10 nm, which is consistent with the SEM and XRD results.

As comparison, the XRD and SEM of Rut-et and Rut-eg were shown in Fig.S1. The samples were still rutile phase, while "coral branch" structures disappeared. The possible reason may be the higher viscosity of DG compared with ethanol and EG. The ion diffusion and nucleation process are hindered in DG solution, which constrains the isotropic growth of the crystal, leading to the branch structures.

The N_2 adsorption/desorption isotherm of Rut-dg exhibited a type Ⅳ isotherm with a H_2 hysteresis loop, demonstrating the mesoporous structures (Fig.S2). The average pore size calculated by BJH method was about 10 nm. The BET surface area of Rut-dg was 228 $m^2\cdot g^{-1}$, which was more than 7 times of Rut-c (32 $m^2\cdot g^{-1}$), indicating the branch structures enhanced the surface area dramatically.

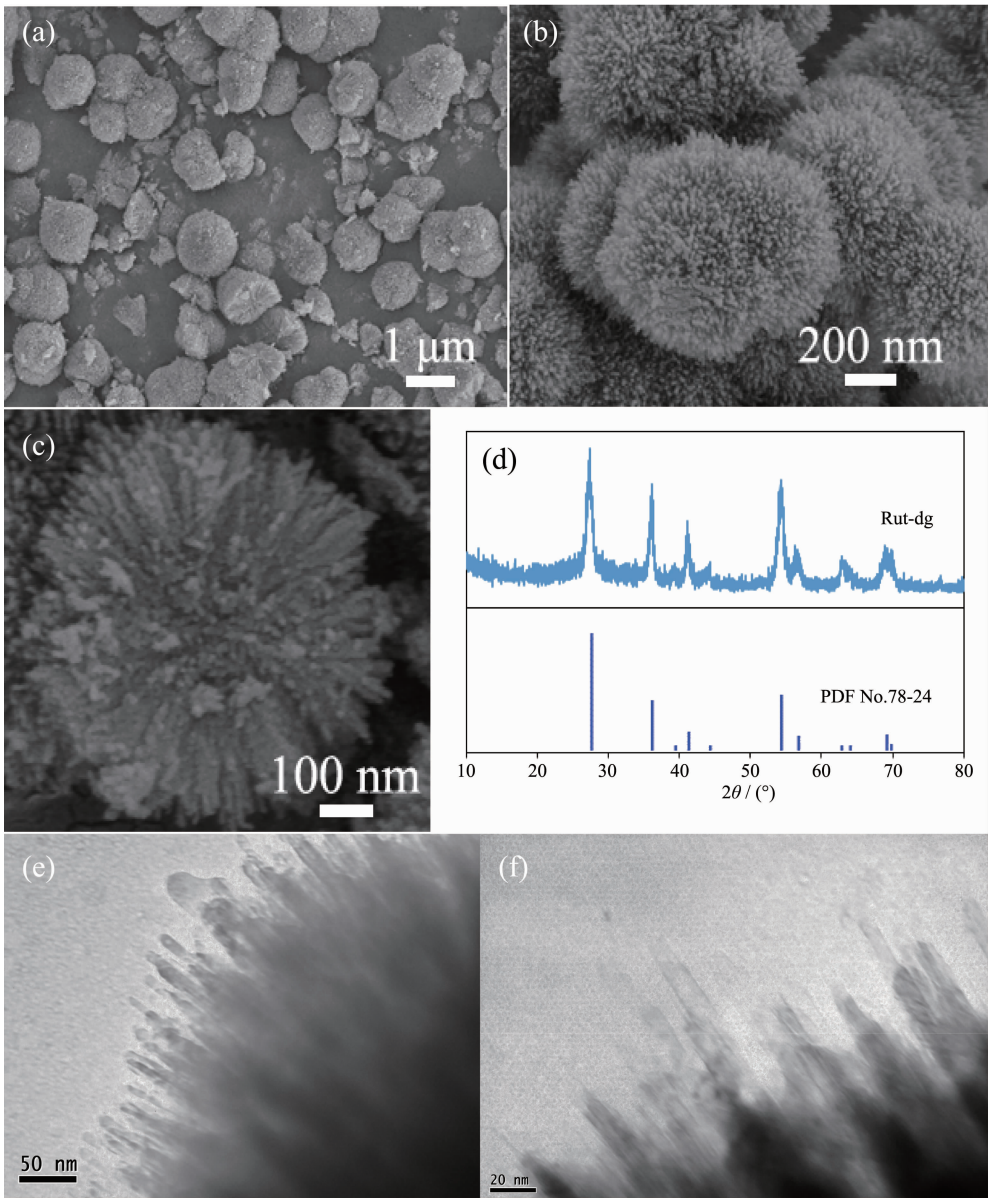

Fig.1　(a~c) SEM images (d), XRD pattern and (e~f) TEM images of Rut-dg samples

2.2　Photocatalytic hydrogen generation experiments

Fig.2 shows the hydrogen production of Rut-dg, Rut-c and P25 samples under UV (Fig.2a) or visible light irradiation (Fig.2b), with an aqueous solution containing 10%(*V*/*V*) TEOA as a scavenger and 3% (*w*/*w*) Pt as a cocatalyst. It can be seen that under UV irradiation, Rut-dg had much higher hydrogen production (about 25 000 μmol·g^{-1}·h^{-1} after 2 h irradiation), which was about 50% higher than commercial P25 and 13 times of Rut-c. Under visible light, only Rut-dg had an obvious photocatalytic activity about 270 μmol·g^{-1}·h^{-1}, while no obvious activities for Rut-c and P25 samples could be detected.

2.3　UV-Vis diffuse reflectance spectroscopy

The optical absorption properties of different samples were investigated by UV-Vis DRS (Fig.3). It can be seen that P25 and Rut-c had no obvious adsorption under visible light (>420 nm). For Rut-dg, the tangent line intersected the wavelength axis at about 421 nm, the values for Rut-c and P25 were 415 and 409 nm, respectively. The maximum absorption wavelength of Rut-dg had only slight redshift. However, it should be noted that the adsorption

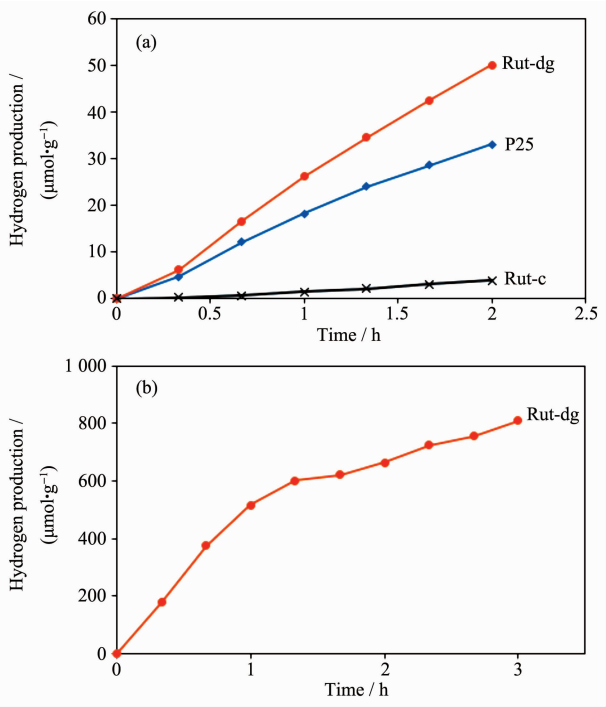

Fig.2 H_2 production of (a) Rut-dg, P25 and Rut-c samples under UV irradiation and (b) Rut-dg sample under visible light

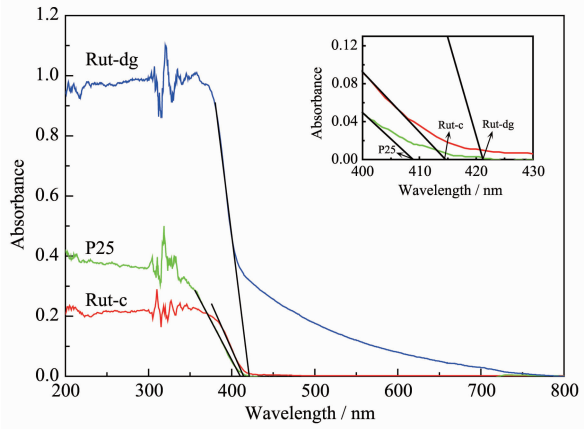

Fig.3 UV-Vis DRS of Rut-dg, P25 and Rut-c

intensity of Rut-dg decreased slowly with the increase of wavelength and still maintained at about 20%~40% of the highest value under visible light range (420~500 nm). Thus, Rut-dg has considerable activity under visible irradiation.

2.4 FT-IR spectra analysis

Organic compounds, such as alcohols (*e.g.*, methanol, ethanol, isopropanol, *etc*.) and organic acids (formic acid, acetic acid, *etc*.), could be used as electron donors in photocatalytic process and promote the hydrogen evolution substantially. FT-IR spectra of Rut-dg and Rut-c were recorded to determine whether existed organics on the surface of the catalysts. As shown in Fig.4, the peaks at ~1 632 cm^{-1} were commonly attributed to the stretching vibrations of C=C bonds or bending vibrations of H-O-H bonds. As no characteristic peaks of C-C, C-H or C-O bonds could be observed in the infrared spectrum, the peaks at 1 632 cm^{-1} should be attributed to absorbed water on the surface of samples. The peaks at 3 379 cm^{-1} should be O-H bending vibration of absorbed water. The FT-IR result showed that no detectable organics existed on the surface of the Rut-dg, which means that the better photocatalytic activity compared with Rut-c should be attributed to the special morphology of Rut-dg sample. It should be noted that the peaks intensity of Rut-dg was much higher than Rut-c. The possible reason should be Rut-dg has coral-like morphology and hydrophilic surface with a large number of hydroxyls on the surface, which leads to capillary condensation, thus more water molecules are absorbed on the surface of Rut-dg.

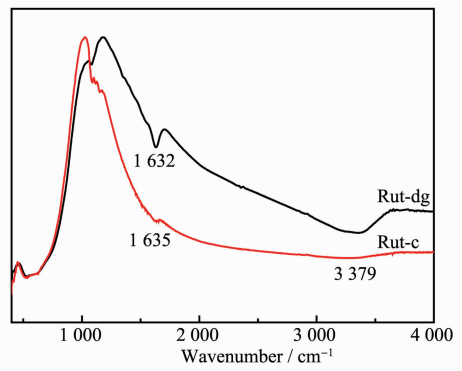

Fig.4 FT-IR of Rut-dg and Rut-c

2.5 Reaction mechanism analysis

The Rut-dg was calcined at 300 ℃ for 1 h before photocatalytic test under UV irradiation. Obvious sintering of the branch structures could be observed in Fig.5a, meanwhile, the BET surface area decreased sharply to 109 $m^2 \cdot g^{-1}$. From the N_2 adsorption-desorption isotherm, it could be clearly seen that the isotherm exhibited a type Ⅱ isotherm, indicating the collapse of the mesoporous structures (Fig.S2). Accordingly the hydrogen production decreased by 15%~25% (Fig.5b), further proving that the coral-like structure is the key

factor for high activity.

The coral-like structure can increase the hydrogen production owing to the following potential reasons (Fig.6):

(1) As discussed in SEM and BET sections, Rut-dg has coral-like structure with high surface area. Compared with Rut-c, the high surface area equates to more surface-active sites in unit volume. The surface-active sites are required for the adsorption of H_2O, which is a key step in photoreactivity between TiO_2 and water[36]. Meanwhile, the coral structures also facilitate the adsorption of water, as discussed above.

(2) Rut-dg coral-like surface with branches diameter was less than 10 nm. According to the literature, when the grain size of titania decreases below 15 nm, the photocatalytic performance will increase abruptly because of quantum size effect and faster charge transfer[37].

(3) The higher surface area of Rut-dg makes more water adsorption and photogenerated carriers excited than Rut-c under same irradiation. Furthermore, the coral structures reduce the transfer distance of photon-generated carriers dramatically and so facilitate the oriented movement and efficient separation of electrons and holes, increase the probability of their reaching the surface without e^--h^+ recombination and enhance the activity remarkably[38].

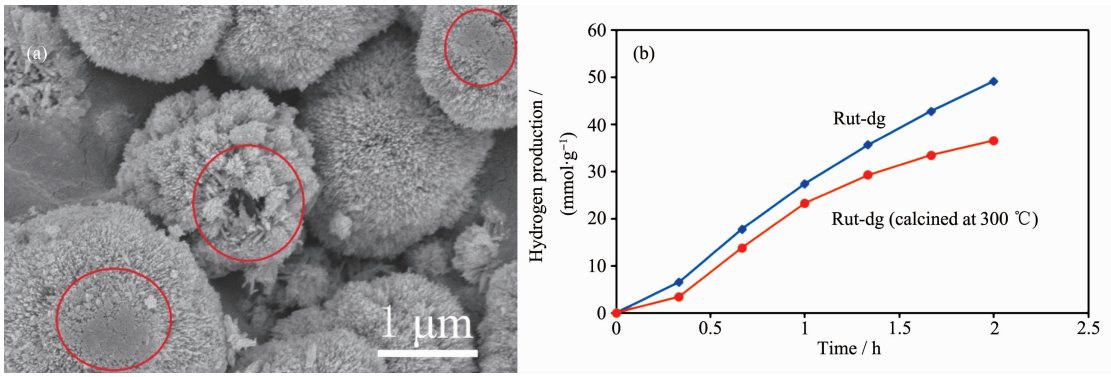

Fig.5　(a) SEM image of Rut-dg calcined at 300 ℃ and (b) hydrogen production under UV irradiation of Rut-dg samples before and after calcination

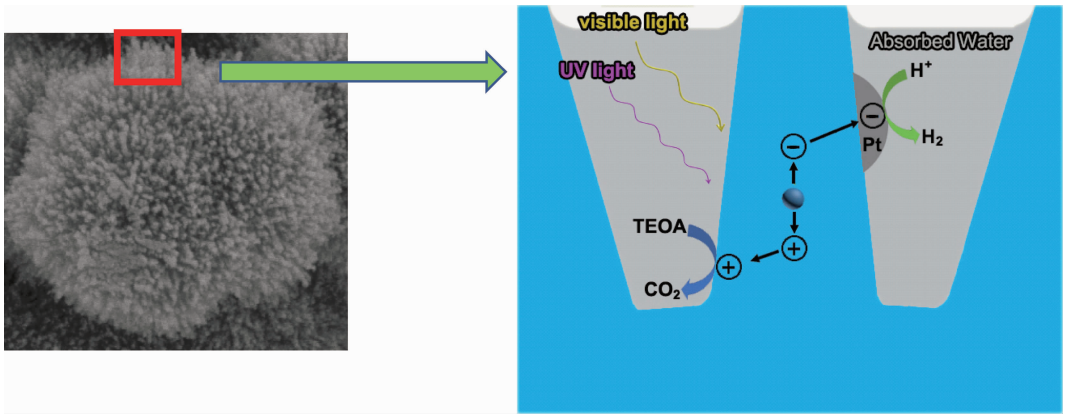

Fig.6　Schematic of the possible hydrogen evolution mechanism over Rut-dg catalyst

3　Conclusions

In summary, the coral-like rutile TiO_2 was synthesized by solvothermal method in DG solution. The coral branch structure increased the surface area of the sample substantially and facilitated the e^--h^+ separation, which lead to its superior performance on photocatalytic water splitting under both UV and visible light.

Acknowledgements: The financial support of the Key Research Project of Social Development of Xuzhou (Grant No.

KC17154) is gratefully acknowledged.

Supporting information is available at http://www.wjhxxb.cn

Reference:

[1] Chu S, Majumdar A. *Nature*, **2012**,**488**:294-303

[2] Xiang Q J, Yu J G, Jaroniec M. *Chem. Soc. Rev.*, **2013**,**41**: 782-796

[3] Maeda K, Domen K. *J. Phys. Chem. Lett.*, **2010**,**1**:2655-2661

[4] Hisatomi T, Kubota J, Domen K. *Chem. Soc. Rev.*, **2014**,**43**: 7520-7535

[5] Bowker M. *Catal. Lett.*, **2012**,**142**:923-929

[6] Chen X B, Shen S H, Guo L J, et al. *Chem. Rev.*, **2010**,**110**: 6503-6570

[7] Fujishima A, Honda K. *Nature*, **1972**,**238**:37-38

[8] Guayaquil-Sosa J F, Serrano-Rosales B, Valades-Pelayo P J, et al. *Appl. Catal. B*, **2017**,**211**:337-348

[9] Wu M H, Zhang M, Lv T, et al. *Appl. Catal. A*, **2017**,**547**: 96-104

[10]Xiao Y, Yu X, Gao Y, et al. *Catal. Commun.*, **2017**,**102**:1-4

[11]Sui Y L, Liu S B, Li T F, et al. *J. Catal.*, **2017**,**353**:250-255

[12]Irfan R M, Jiang D C, Sun Z J, et al. *J. Catal.*, **2017**,**353**: 274-285

[13]Imran M, Yousaf A B, Kasak P, et al. *J. Catal.*, **2017**,**353**: 81-88

[14]Bharatvaj J, Preethi V, Kamnani S. *Int. J. Hydrogen Energy*, **2018**,**43**:3935-3945

[15]Cui E T, Meng Q Q, Ge C Y, et al. *Catal. Commun.*, **2018**,**103**: 29-33

[16]Chava R K, Do J Y, Kang M. *J. Alloys Compd.*, **2017**,**727**: 86-93

[17]Yu K, Zhang C X, Chang Y, et al. *Appl. Catal. B*, **2017**,**200**: 514-520

[18]Qu Z P, Rong Y, Tang L, et al. *Mol. Catal.*, **2017**,**441**:10-20

[19]Sadovnikov S I, Kozlova E A, Gerasimov E Y, et al. *Catal. Commun.*, **2017**,**100**:178-182

[20]Lee W P C, Gui M M, Tan L L, et al. *Catal. Commun.*, **2017**,**98**:66-70

[21]Kumar D P, Park H, Kim E H, et al. *Appl. Catal. B*, **2018**, **224**:230-238

[22]Ding N, Zhang L S, Zhang H Y, et al. *Catal. Commun.*, **2017**,**100**:173-177

[23]Gao J T, Wang Y, Zhou S J, et al. *ChemCatChem*, **2017**,**9**: 1708-1715

[24]Zhu Y P, Ren T Z, Yuan Z Y. *ACS Appl. Mater. Interfaces*, **2015**,**7**:16850-16856

[25]Han Q, Wang B, Gao J, et al. *ACS Nano*, **2016**,**10**:2745-2751

[26]Zhang J Y, Wang Y H, Jin J, et al. *ACS Appl. Mater. Interfaces*, **2013**,**5**:10317-10324

[27]Ma Y, Wang X L, Jia Y S, et al. *Chem. Rev.*, **2014**,**114**: 9987-10043

[28]Zhang J, Xu Q, Feng Z C, et al. *Angew. Chem. Int. Ed.*, **2008**,**47**:1766-1769

[29]Liu Y X, Wang Z L, Huang W X. *Appl. Surf. Sci.*, **2016**, **389**:760-767

[30]Liu Y X, Wang Z L, Wang W D, et al. *J. Catal.*, **2014**,**310**: 16-23

[31]Wahab A K, Ould-Chikh S, Meyer K, et al. *J. Catal.*, **2017**, **352**:657-671

[32]Wang P F, Zhou Q X, Xia Y G, et al. *Appl. Catal. B*, **2018**, **225**:433-444

[33]Shahi S K, Kaur N, Sandhu S, et al. *J. Sci.*: *Adv. Mater. Devices*, **2017**,*2*:347-353

[34]Hua X S, Zhang Y J, Ma N H, et al. *J. Hazard. Mater.*, **2009**,**172**:256-261

[35]Wang D D, Shan Z Q, Na R, et al. *J. Power Sources*, **2017**, **337**:11-17

[36]Nowotny J, Bak T, Nowotny M, et al. *J. Phys. Chem. B*, **2006**,**110**:18492-18495

[37]Ren H J, Koshy P, Chen W F, et al. *J. Hazard. Mater.*, **2017**,**325**:340-366

[38]Chen X Y, Yu T, Fan X X, et al. *Appl. Surf. Sci.*, **2007**, **253**:8500-8506